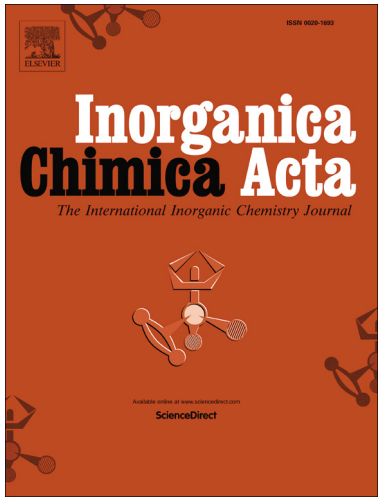

Synthesis, characterization, DNA binding and cytotoxicity of fluoro-dipyrrin based arene ruthenium (II) complexes

Rajendra Prasad Paitandi, Roop Shikha Singh, Sujay Mukhopadhyay, Gunjan Sharma, Biplob Koch, Pratap Vishnoi, Daya Shankar Pandey

PII: S0020-1693(16)30095-0
DOI: http://dx.doi.org/10.1016/j.ica.2016.03.003
Reference: ICA 16938

To appear in: *Inorganica Chimica Acta*

Received Date: 23 January 2016
Revised Date: 2 March 2016
Accepted Date: 3 March 2016

Please cite this article as: R.P. Paitandi, R.S. Singh, S. Mukhopadhyay, G. Sharma, B. Koch, P. Vishnoi, D.S. Pandey, Synthesis, characterization, DNA binding and cytotoxicity of fluoro-dipyrrin based arene ruthenium (II) complexes, *Inorganica Chimica Acta* (2016), doi: http://dx.doi.org/10.1016/j.ica.2016.03.003

Synthesis, characterization,DNA binding and cytotoxicity of fluoro-dipyrrin based arene ruthenium(II) complexes

Rajendra Prasad Paitandi[a], Roop Shikha Singh[a], Sujay Mukhopadhyay[a],Gunjan Sharma[b], Biplob Koch[b*],Pratap Vishnoi[c],Daya Shankar Pandey[a]*

[a]Department of Chemistry, Institute of Science, Banaras Hindu University, Varanasi – 221 005 (U.P.) India.

[b]Department of Zoology, Institute of Science, Banaras Hindu University, Varanasi – 221 005 (U.P.) India

[c]Department of Chemistry, Indian Institute of Technology, Bombay, Powai, Mumbai– 400076, India.

Abstract

Synthesis of four new areneruthenium(II) complexes [(η^6-$C_{10}H_{14}$)RuCl(MFPdpm)] (**1**); [(η^6-$C_{12}H_{18}$)Ru-Cl(MFPdpm)] (**2**); [(η^6-$C_{10}H_{14}$)RuCl(PFPdpm)] (**3**) and [(η^6-$C_{12}H_{18}$)RuCl(PFPdpm)] (**4**)containingdipyrrin ligands5-(4-fluoro)phenyldipyrromethene (MFPdpm) and 5-(penta-fluoro)phenyldipyrromethene (PFPdpm) have beendescribed. The ligands and complexes have been thoroughly characterized by elemental analyses,spectroscopic studies (ESI-MS, IR, ^{1}H, ^{13}C NMR, UV−vis.) and structure of the representative complex **4** determined by X-ray single crystal analyses. DNA binding activities of **1**–**4** havebeen investigated byUV−vis and fluorescence spectroscopy and their binding through the minor groove of DNA has been established by molecular docking studies. The complexes **1**–**4** exhibit significant cytotoxicity toward human lung cancer cell line (A549). Cytotoxicity, morphological changes, and apoptosis studies have been evaluated through MTT assay, Hoechst 33342/PI staining, and cell cycle analysis by fluorescenceactivated cell sorting (FACS). *In vitro* antitumor activity and cytotoxicity of the complexes lie in the order **4** >**3**>**2** >**1.**

*Corresponding author. E-mail: dspbhu@bhu.ac.in; Tel.: + 91 542 6702480; Fax: + 91 542 2368174.

1. Introduction:

Since successful application of *cis*-platin and its derivatives in the treatment of a broad spectrum of cancer numerous platinum [1–3] and non-platinum based metal complexes have fascinated many research groups [4–12]. Although,*cis*-platin is one of the most active anticancer drugs, its usage is limited due to high toxicity, drug selectivity, intrinsic and acquired resistance. To overcome the disadvantagesof platinum based drugs,attempts are being made to develop alternative metal-based antitumor agents [4–14].In this context, ruthenium based complexes have drawn special attention andamong these KP1019 and NAMI-A have shown great promise owing to their therapeutic potential, low toxicity, and activity against primary tumors and metastases [15–18]. Meanwhile, intercalators have been target of many studies because intercalation distorts the helical structure of DNA and causes inhibition of replication enzymes [19–24]. Thus in the burgeoning area of DNA intercalation studies, ruthenium based intercalators have been imperative due to their specific redox and photophysical properties [19–21].Further,antitumor activity of many Ru(II)-arene complexes has been related to their enhanced DNA binding affinity, through covalent and/or non-covalent interactions [22–24].

In addition, dipyrrins present conjugated π-systems consisting of two pyrrolic units andform a variety of metal complexes which find applications in diverse areas such as dye-sensitized solar cells, biological stains/probes, light harvester and anticancer agents [25–31]. Recently we have synthesized some stable neutral homo/heteroleptic Ru(II), Rh(III), and Ir(III) dipyrrinato complexes exhibiting enhanced anticancer activity[29–31]. To explore possible modes of intercalation we have supplemented the dipyrrin core with various substituents ranging from thioethers, ferrocenyl to 2-methoxypyridyl etc. [29–31].Further, to enable covalent interaction with biological targets, modern day drugs are usually equipped with a halide leaving group particularly, fluorine as it allows simultaneous modulation of the electronic, lipophilic and steric parameters [32 –33]. In this directionconsidering wide range of biological functions numerous fluorinated organic molecules have been developed.

Furthermore, fluorinated anti-cancer agents have attracted huge interest towards development of new therapies for cancer treatment [34–35].Therefore,in view of the advancements made toward development of potential bioorganometallic compoundswe wished to develop some arene ruthenium (II) complexes based on fluorinated dipyrrin core which could be potential anticancer

agents.Through this contribution we presentfour half-sandwich complexes of the type [Ru(η^6-arene)-(L)Cl], where arene is *p*-cymene (**1**, **3**) and hexamethylbenzene (**2**, **4**) and L is 4-fluorophenyldipyrrins (MFPdpmH) and 1,2,3,4,5-penta-fluorophenyldipyrrins(PFPdpmH)and their anticancer activity (Scheme 1). Also, we describe herein anticancer activity of the synthesized complexes and structure-activity relationship with different fluorodipyrrinato ligands and arene moiety.

.

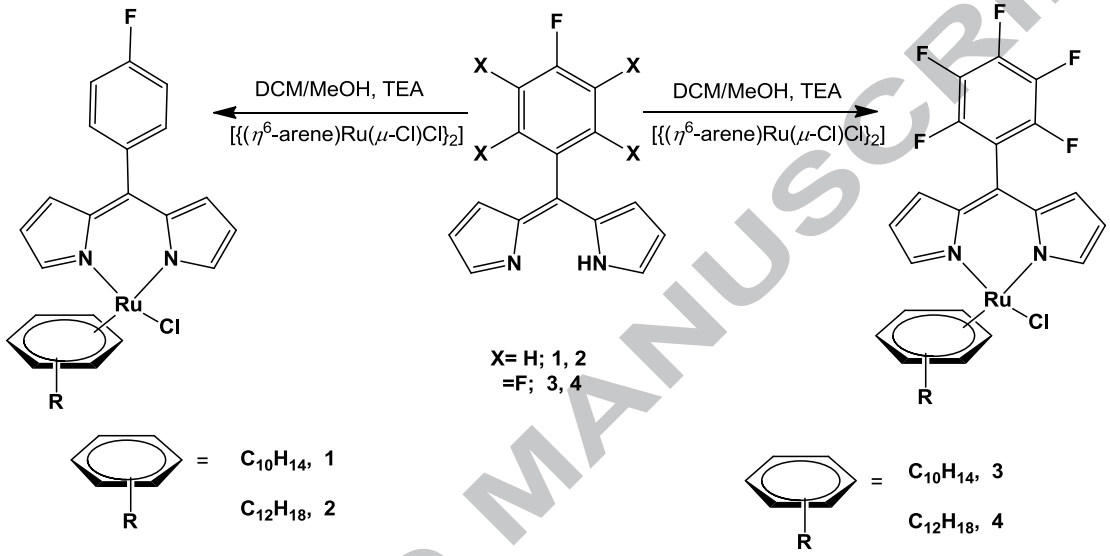

Scheme 1. Synthesis of complexes **1**–**4**

2.Experimental Section

2.1.Reagents.

Reagent grade chemicals were used throughout.Solvents were dried and distilled following literature procedures and reactions carried out under nitrogen atmosphere [36]. Metal chlorides ($RuCl_3 \cdot xH_2O$), agarose,α-terpinene, 2,3-dichloro-5,6-dicyano-1,4-benzoquinone (DDQ), 4-(fluoro)benzaldehyde, pentafluorobenzaldehyde, and pyrrole were procured from Sigma Aldrich Chemical Co.and used without further purifications. 3-(4, 5-dimethylthiazol-2-yl)-2,5-diphenyltetrazolium bromide (MTT), fetal bovine serum (FBS) and RPMI-1640, were purchased from Hi-Mediaand ethidium bromide (EB) from Loba Chemie, while acridine orange (AO) from Sisco Research Laboratory (SRL), Mumbai, India. Triton X-100 and other chemicals of analytical grades were purchased from Lobachemie Pvt. Ltd., India and RNAse was obtained from GeNie, Merck, India. Propidium iodide was purchased from Calbiochem, USA. Lung

cancer cell line (A549) was obtained from National centre for cell science (NCCS) Pune. Calf thymus (CT DNA) was purchased from Bangalore Genei, India and *cis*-platin 50 mg/50 ml was obtained from Cipla with the name *cis*-platin injection BP Cytoplatin-50 Aqueous (Each 50 ml vial contains: *cis*-platin IP 50 mg, sodium chloride IP 0.9% w/v and water for injection IP to 50 ml).The precursor complexes [{(η^6-arene)Ru(μ-Cl)Cl}$_2$] (η^6-arene =$C_{10}H_{14}$, $C_{12}H_{18}$) [37–38]and ligands 5-(4-fluoro) phenyldipyrromethane (MFPdpmH), 5-(pentafluoro)phenyldipyrro-methane (PFPdpmH)wereprepared and purifiedbyliteratureprocedures [39].

2.2. General Methods.

Elemental analyses for C, H and N were performed on a Euro-E 3000 Elemental Analyzer.Infrared and electronic absorption spectra were acquired on a PerkinElmer Spectrum Version 10.03.05 FT-IR and Shimadzu UV-1601 spectrophotometer respectively. ^{1}H (300 MHz) and ^{13}C (75.45 MHz) NMR spectra were obtained on a JEOL AL300 FT-NMR spectrometer using tetramethylsilane (TMS) as an internal reference. Fluorescence spectra were obtained on PerkinElmer LS-55 spectrofluorimeter equipped with a xenon lamp in a 10.0 mm quartz cell with excitation and emission slit widths of 10 and 5 nm, respectively. Fluorescence microscopic images were taken on EVOS FL cell imaging system and electrospray ionization mass spectrometric data were obtained on a micrOTF-Q IImass spectrometer.

2.3. Synthesis

Synthesis of [(η^6-$C_{10}H_{14}$)RuCl(MFPdpm)] ***(1)***

DDQ (0.114 g, 0.50 mmol) dissolved in benzene (20 ml) was added dropwise with stirring to an ice cooled solution ofMFPdpmH (0.120 g, 0.50 mmol) in CH_2Cl_2 (50 mL)and reaction mixture stirred for an additional 1 h. After completion of the reaction (monitored by TLC) solvent was removed under reduced pressure. Resulting residue was dissolved in CH_2Cl_2/MeOH (70 mL; 1:1 v/v) and treated successively withtriethylamine (1.0 mL) and dimeric complex [{(η^6-$C_{10}H_{14}$)Ru(μ-Cl)Cl}$_2$] (0.153 g, 0.25 mmol). The reaction mixture wasfurther stirred for ~4 h at room temperature. The solvent was removed under reduced pressure and resulting residue was purified bycolumn chromatography (SiO_2, CH_2Cl_2 with 2% MeOH) to afford complex **1** as a red solid. Yield: 50% (0.254 g). Anal. Calc for $C_{25}H_{24}N_2FClRu$: C, 60.77; H, 5.41; N, 12.89. Found: C, 60.71; H, 5.36; N, 12.84%. ^{1}H NMR ($CDCl_3$, δ ppm): 1.08 (d, 6H, J = 6.9 Hz, CH(C$\underline{H}_3$)$_2$), 2.17 (s, 3H, C$\underline{H}_3$), 2.43 (m, 1H, C$\underline{H}$(CH$_3$)$_2$), 5.27 (s,

4H,$C_6\underline{H}_4$), 6.47 (d, 2H, *J* = 4.2 Hz, pyrrole), 6.55 (d, 2H, *J* = 3.6 Hz, pyrrole), 7.0 (t, 2H, *J* = 8.7 Hz,phenyl), 7.35 (t, 2H, *J* = 8.7 Hz,phenyl), 8.01 (s, 2H, pyrrole).^{13}C NMR ($CDCl_3$, δ ppm): 22.06 ($CH(\underline{C}H_3)_2$), 29.0 ($\underline{C}H_3$), 30.6 ($\underline{C}H(CH_3)_2$), 53.1 (*C- meso*, dipyrrin), 84.5, 84.8, 108.2, 118.9,130.5, 155.4, 180.5. ESI-MS. (Calcd, found, *m/z*) 473.0967, 473.1000 $[M–Cl]^+$. IR (KBr pellets, cm^{-1}): 1027, 1249, 1345, 1376, 1466, 1550.UV–vis. (*c*, 10 μM; EtOH:H_2O, 1:1, v: v; *p*H ~7.3; λ_{max} nm, ε M^{-1} cm^{-1}): 491 (2.8 $\times10^4$), 430 (1.2 $\times10^4$), 315 (0.7 $\times10^4$), 221 (2.4 $\times10^4$)

Synthesis of [(η^6-$C_{12}H_{18}$)RuCl(MFPdpm)] ***(2)***

This complex was prepared following the above procedure for **1** except that [{(η^6-$C_{12}H_{18}$)Ru(μ-Cl)Cl}$_2$] (0.167 g, 0.25 mmol) was used in place of [{(η^6-$C_{10}H_{14}$)Ru(μ-Cl)Cl}$_2$] (0.153 g, 0.25 mmol). Yield: 56% (0.230 g). Anal. Calc for $C_{27}H_{28}N_2FClRu$: requires: C, 62.71; H, 5.57; N, 10.75. Found: C, 62.67; H, 5.48; N, 10.80%.^{1}H NMR ($CDCl_3$, δ ppm): 1.9 (s, 18H, $C\underline{H}_3$), 6.48 (d, 2H, *J* = 3.9 Hz, pyrrole), 6.64 (d, 2H, *J* = 4.2 Hz, pyrrole), 7.0 (t, 2H, *J* = 8.4 Hz,phenyl), 7.35 (t, 2H, *J* = 8.4 Hz,phenyl), 8.01 (s, 2H, pyrrole). ^{13}C NMR ($CDCl_3$, δ ppm): 29.6 ($\underline{C}$H3,), 55.4 (*C- meso*, dipyrrin), 114.4, 114.6, 116.9, 119.4, (dipyrrin) 132.3, 132.9, 143.9, 148.7, 154.1 (Phenyl ring). ESI-MS. (Calcd, found, *m/z*) 501.12, 501.10$[M–Cl]^+$. IR (KBr pellets, cm^{-1}): 1028, 1250, 1345, 1375, 1429, 1551. UV–vis. (*c*, 10 μM; EtOH:H_2O, 1:1, v: v; *p*H ~7.3; λ_{max} nm, ε M^{-1} cm^{-1}): 438 (1.5 $\times10^4$), 322 (1.1 $\times10^4$), 261 (1.0 $\times10^4$).

Synthesis of [(η^6-$C_{10}H_{14}$)RuCl(PFPdpm)] ***(3)***

It was prepared following the above procedure for **1** except thatPFPdpmH (0.156 g, 0.5 mmol) was used in place of MFPdpmH (0.120 g, 0.50 mmol) Yield: 48% (0.292 g). Anal. Calc for $C_{27}H_{24}N_2F_5ClRu$, requires: C, 53.34; H, 3.98; N, 4.61. Found C, 53.28; H, 3.94; N, 4.57%.^{1}H NMR ($CDCl_3$, δ ppm): 1.09 (d, 6H, *J* = 6.6 $CH(C\underline{H}_3)_2$), 2.14 (s, 3H,$C\underline{H}_3$), 2.55 (m, 1H,$C\underline{H}(CH_3)_2$), 5.25 (d, 2H, *J* = 5.7Hz, $C_6\underline{H}_4$), 5.33 (d, 2H, *J* = 5.7Hz, $C_6\underline{H}_4$) ,6.51 (s, 4H, pyrrole),8.02 (s, 2H, pyrrole).^{13}C NMR ($CDCl_3$, δ ppm): 30.8 (*C- meso*, dipyrrin), 30.5$\underline{C}H(CH_3)_2$),21.9($\underline{C}H_3$) , 18.2 $CH(\underline{C}H_3)_2$, 99.7, 103.4, 119.6, 134.2, 156.35, 156.36 (dipyrrin).ESI-MS. (Calcd, found, *m/z*) 573.0903, 573.0865 $[M–Cl]^+$. IR (KBr pellets, cm^{-1}): 987, 1026, 1248, 1343, 1377, 1496, 1518, 1567. UV–vis (*c*, 10 μM; EtOH:H_2O, 1:1, v: v; *p*H ~7.3; λ_{max} nm, ε M^{-1} cm^{-1}): 499 (0.77 $\times10^4$), 441 (0.47 $\times10^4$), 303 (0.24 $\times10^4$), 221 (0.97 $\times10^4$).

Synthesis of [(η^6-$C_{12}H_{18}$)RuCl(PFPdpm)] ***(4)***

It was prepared following the above procedure for **2** except that PFPdpmH (0.156 g, 0.5 mmol) was used in place of MFPdpmH (0.120 g, 0.50 mmol) Yield: 52% (0.237 g). Anal. Calc for $C_{27}H_{24}N_2F_5ClRu$: requires: C, 53.34; H, 3.98; N,4.61. Found: C, 53.29; H, 3.93; N, 4.55%. ^{1}H NMR ($CDCl_3$, δ ppm): 1.91 (s, 18H, C*H*$_3$), 6.45 (d, 2H, J = 4.2 Hz,pyrrole), 6.53 (d, 2H, J = 4.2 Hz pyrrole), 7.75 (s, 2H, pyrrole), ^{13}C NMR ($CDCl_3$, δ ppm): 15.0 (*C*H3,), 56.9 (*C*- *meso*, dipyrrin), 93.8, 119.2, 130.2, 134.5, 155.7. ESI-MS. (Calcd, found, *m/z*) 545.0590, 545.0550 [M-Cl]$^+$. IR (KBr pellets, cm^{-1}): 988, 1042, 1114, 1441, 1499, 1521, 1594. UV–vis (*c*, 10 μM; EtOH:H_2O, 1:1, v:v; *p*H ~7.3; λ_{max} nm, ε M^{-1} cm^{-1}): 513 (1.40 ×10^4), 453 (1.49 ×10^4), 306 (0.46 ×10^4), 223 (1.71 ×10^4)

2.4. X-ray Structure Determination.

Crystals suitable for X-ray single crystal analyses for **4** were obtained by slow diffusion of hexane over a dichloromethane solution of the complex. X-ray data for**4**were collected on a Rigaku Saturn 724+ CCD diffractometer with a fine-focus 1.75 kW sealed tube Mo Kα (λ = 0.71075 Å) X-ray source.Structures were solved by direct methods (SHELXS 97) and refined by full-matrix least squares on F^2 (SHELX 97)[40].Disordered solvent molecules were removed by SQUEEZE command in PLATON [41–42]. All the non-H atoms were treated anisotropically. The H-atoms attached to aromatic carbon were included as fixed contribution and geometrically calculated and refined using SHELX riding model. Intermolecular interactions and stacking distances were analysed by using computer program PLATON.

2.5. DNA Binding Studies.

UV–vistitration studies have been performedby gradual additions of increasing concentrations of CT DNA (Na-phosphate buffer solution, *p*H 7.2) to a solution of the complexes **1**–**4**[fixed concentration,10 μM, ethanol/water (EtOH/H_2O), 1:1, v/v].Absorbance of the stock solution of CT DNA at 260 and 280 nm gave a ratio of 1.9, suggesting the DNA to beadequately free of proteins.Concentration of DNA was determined using the molar extinction coefficient of 6600 M^{-1}cm^{-1} at 260 nm. An analogous method has been used for fluorescence studies also. Ethidium bromide (EB) displacement experiments were executed by addition of **1**–**4**to an aqueous solution of EB-DNA and simultaneous monitoring of the changes influorescence intensity of emission maxima at 602 nm (λ_{ex}, 525nm).

2.6. Partition Coefficient Determination.

Lipophilicity of the complexes under study was evaluatedby“Shake flask” method in octanol/water phase partitions as described elsewhere [29].

2.7. Molecular Docking.

Molecular docking studies on **1**–**4** have been performed using HEX 6.1 software and Q-site finder which is an interactive molecular graphics program for interaction and docking calculations and to classify possible binding site of the biomolecules [43].The DFT calculations were carried out using Gaussian 09 program, B3LYP method [44]. Geometry of the complexes **1**–**4**were optimized with standard 6–31G** basis sets for C, H, N, O, and Cl and LANL2DZ for Ru with effective core pseudo potential for metal[45–46]. The coordinates of metal complexes were taken from its optimized structure as a .mol file and transformed to PDB format using CHIMERA 1.5.1 software.Crystal structure of B-DNA (PDB ID: 1BNA) was recovered from the protein data bank (http://www.rcsb.org./pdb). Visualization of the docked structures has been performed by Discovery Studio 3.5 software. The by default parameters were used for docking calculations with correlation type shape only, FFT mode at 3D level, grid dimension was 6 with receptor range 180 and ligand range 180 with twist range 360 and distance range 40.

2.8. Cytotoxicity and proliferation assay by MTT Assay.

The MTT assay is a quantitative, sensitive and reliable colorimetric assay generally used for assessing viability and proliferation of the cells. In this assay mitochondrial dehydrogenase enzymes of live cells convert the yellow water soluble substrate, 3-(4,5-dimethylthiazol-2-yl)-2,5-diphenyltetra-zolium bromide (MTT) into a purple formazan crystal product which is insoluble in water or medium[47].

MTT of working concentration of 5 mg/ml was prepared in 1X phosphate buffered saline (PBS) and 10µL added into each well of 96 well cell culture plates where 10,000 cells were seeded in each well except the blank with different concentrations of **1**–**4**and incubated for 24 h at 37 °C and in 5% CO_2 atmosphere. After adding MTT the cells were again incubated for 2 h at 37 °C. Mitochondrial dehydrogenase of the viable cells cleave tetrazolium ring of the substrate (MTT) and produce purple formazan crystal which is insoluble in medium, after that 100µL of DMSO was added to dissolve the formazan crystals and incubated for 30 minutes at 37 °C and absorbance was measured spectrophotometrically in ELISA plate reader at 570 nm. All the

experiments were carried out in three to five replicates and IC_{50} value for each compound estimated.

2.9. Analysis of cell/nucleus morphology with Hoechst 33342/PI staining.

Cell death is discriminated into two main forms, apoptosis and necrosis. In contrast to necrosis, apoptosis is a programmed and regulated pathway of cell death [48]. Morphological hallmarks of apoptosis in the nucleus are chromatin condensation and nuclear fragmentation[49]. This condensation and fragmentation can be followed byfluorescence microscopy after staining with DNA binding fluorescence dyes.Hoechst and PI double staining provide a fast and suitable assay for nucleus morphology and apoptosis. Hoechst binds in the minor groove of double stranded DNA preferably AT rich region while PI intercalates between the bases without any sequence preference. PI is normally used to identify dead cells as it is membrane impermeable and gets excluded from viable cells while Hoechst dye is permeable to the cell membrane and binds to DNA in live or fixed cells.

In the present study cells were seeded in 6 well plates and kept for 24 h at 37 °C in a humidified atmosphere of 5% CO_2. After that cells were treated with different concentrations (15, 20 and 25μM) of complex **4** for 24 h. Subsequently, cells were washed with PBS and stained with Hoechst (10μg/mL) and propidium iodide (10μg/mL) solution. These were then washed with PBS and images were taken in inverted fluorescent microscope in red and blue channel.

2.10. FACS analysis with PI staining.

Besides other typical features apoptotic cells are characterized by DNA fragmentation and consequently loss of nuclear DNA content. Use of a fluorochrome such as PI(propidium iodide) that is capable of binding and labeling DNA makes it possible to get a rapid and precise evaluation of cellular DNA content by flow cytometric analysis and subsequent identification of hypodiploid cells[50].

The DNA content during cell cycle was evaluatedby flow cytometry. 1×10^5 A549 lung cancer cells were seeded in 6 well plates and kept at 37 °C in a humidified atmosphere of 5% CO_2. After that these were treated with three different concentrations (15, 20 and 25 μM) of complex **4** for 24 h in DMEM medium with 10% FBS. After 24 h the treated cells were washed, trypsinised and fixed in ice cold 70% ethanol and incubated for overnight at -20^oC. Then the cells were washed twice in PBS, 500 μL of staining solution [460 μL of 0.1% (v/v) Triton x-100

solution, 20 µL of PI (1 mg/mL) solution and 20 µL of RNase (10 mg/mL in MQ water)] was added in each sample and incubated for 40 minutes at 37^{o}C in the dark and samples evaluated by a flow cytometer.

3. Results and Discussion

3.1. Synthesis and Characterization

Ligands5-(4-fluoro)phenyldipyrromethane (MFPdpmH) and 5-(pentafluoro)phenyldipyrro-methane (PFPdpmH)werepreparedin reasonably good yield (70–75%) by one-pot solvent free reaction of the respective aldehydes (4-fluorobenzaldehyde/ pentafluorobenzaldehyde) with an excess of pyrrole in presence of catalytic amounts of trifluoroacetic acid (TFA) [39]. The complexes **1**–**4**,*viz*. [(η^6-$C_{10}H_{14}$)RuCl(MFPdpm)], **1**; [(η^6-$C_{12}H_{18}$)RuCl(MFPdpm)],**2**; [(η^6-$C_{10}H_{14}$)RuCl-(PFPdpm)], **3** and [(η^6-$C_{12}H_{18}$)RuCl(PFPdpm)],**4** were synthesized by reaction of chloro bridged dimeric arene ruthenium precursors [{(η^6-arene)Ru(μ-Cl)Cl}$_2$] (η^6-arene = $C_{10}H_{14}$,$C_{12}H_{18}$) with MFPdpm/PFPdpm obtained *in-situ*by oxidation of respective dipyrro-methanes MFPdpmH-/PFPdpmH with DDQ in CH_2Cl_2/CH_3OH (1:1, v/v) in presence of triethylamine at room temperature.Simple scheme showing synthesis of the complexes isdepicted in **Scheme 1**.

The complexes under investigation are non-hygroscopic, orange-red crystalline solids, soluble in common organic solvents like methanol, ethanol, acetone, dichloromethane, chloroform, dimethylformamide, dimethylsulfoxide, and partially soluble in diethyl ether, petroleum ether, hexane and stable in air as well as in solution. All the complexes have been characterized satisfactorily by elementalanalyses and spectral studies [ESI-MS, IR, ^{1}H, ^{13}C NMR, UV–vis]. IR spectra of **1**–**4** displayed diagnostic bands due to pyrrolic ring ν(C=N_{pyr}) vibrations at (1590, **1**; 1591, **2**; 1521, **3**; 1520, **4** cm^{-1}) which slightly shifted towards lower frequency than the free ligand (1596 cm^{-1},MFPdpmH, 1559 cm^{-1},PFPdpmH) indicating coordination of the ligand to metal center [29–31].

3.2. NMR Spectral Studies

The NMR spectra of dipyrromethanes and complexes **1**–**4**have been acquired in $CDCl_3$and resulting data is summarized in the experimental section. ^{1}H NMR spectra of MFPdpmH-/PFPdpmHexhibited peakscorresponding to*meso*(5.44, MFPdpmH; 5.90ppm, PFPdpmH),pyrrolic [5.88, 6.15, 6.67, and 7.90 (br, N*H*), MFPdpmH; 6.02, 6.16,6.72, 8.15 ppm

(br, N*H*), PFPdpmH] and aromatic protons (6.98, 7.17, MFPdpmH) [39].^{1}H NMR spectra of **1**–**4**displayed loss of *meso*-subsituted (–CH) and –N*H* protonssuggesting oxidation of the ligandwhile pyrrolic and phenyl ring protons resonated at their usual positionwith asmalldownfield shift (Figure S1–S4, SI). The change in peak position and integrated intensity clearly indicated coordination of the ligand with metal centerand thereby formation of dipyrrin complexes[29-31].Further, arene protons in **1**–**4**displayed an up-field shift relative to respective precursor complexes[29–31]. In the ^{1}H NMR spectra of **1** and **3**the protons due to arene ring exhibited a little upfield shift [1.08 (CH(C$\underline{H}_3$)$_2$), 2.17 (C$\underline{H}_3$), 2.43(C$\underline{H}$(CH$_3$)$_2$), 5.27 (C$_6\underline{H}_4$), (merged peak) **1**; 1.09 (CH(C$\underline{H}_3$)$_2$), **3**; 2.14 (C$\underline{H}_3$), 2.55 (C$\underline{H}$(CH$_3$)$_2$), 5.25 ppm (merged peak) C$_6\underline{H}_4$), **3**]relative to precursor complexes. Shift in the position of MFPdpmH/PFPdpmH and arene protonsfurther suggested complexation of the ligands with metal center and formation of respective complexes. ^{13}C NMR spectral data of **1-4** further supported formation of these complexes and their proposed formulations and is consistent with earlier reports[29–31].

3.3. Mass spectral studies.

The composition and stability of complexes has been studied by ESI–MS spectral studies. In their positive ESI mass spectra **1**–**4** showedmajor peaks due to cationic fragment [(arene)-Ru(dpm)]$^{+}$ generated by loss of the Cl^{-} (*m/z* found 473.10; **1**, 501.10**2**;545.05**3**; 573.08, **4**) from the respective complexes. The results clearly suggested that chloro (Cl^{-}) group is labile and possibly replaced by targeted biomolecules (Figure S5–S8, SI) [51].

3.4. Crystal Structure.

Crystalstructure of **4** has been determined by X-ray single crystal data. It crystallizes in monoclinic system with $P2_1/n$space group. Details about the data collection, solution and refinement have been given in the experimental section and (Table 1). Pertinent view along with partial atom numbering scheme is shown in (Fig. 1) and important bond length and angles are summarized in (Table 2). The Ru(II) center in this complex adopted typical piano stool geometry with two positions occupied by pyrrolic nitrogen (N1, N2) from PFPdpm, the chloro (Cl1) group and arenering bonded in η^6-manner[29–31].The ruthenium to pyrrolic nitrogen bond distances are identical [Ru–N1, 2.07 Å; Ru–N2, 2.08 Å], while Ru–Cl bond distance (Ru–Cl1) is 2.40 Å, these are normal and comparable to other closely related complexes[29–31].The bond angles N–Ru–N and N–Ru–Cl about metal center are close to 90° [N1–Ru–N2, 83.54°; N1–Ru–Cl1,

87.18°; N2−Ru−Cl1, 87.18°] (Table 2). The arene ring is symmetrically bonded to the metal ion with an average Ru–C bond distance of 2.16 Å [range, 2.135–2.175 Å]. The carbon atoms in arene ring are planar and distance between ruthenium and centroid of the hexamethylbenzene ring is 1.69 Å, (**4**) which is normal and consistent with other arene ruthenium complexes [29–31].

3.5. Electronic absorption spectroscopy.

UV−vis absorption spectra of **1**–**4** were recorded in EtOH: H_2O, *c*, 10 μM; 1:1, v/v; *p*H ~7.3(Fig. 2). The absorption spectra exhibited three major bands, an intense low energy band at ~ 500 nm [489, **1**; 491, **2**; 494, **3**; 513 nm **4**] corresponding to π-π* charge transfer from conjugated dipyrrin core, and low intensity bands at ~ 440 nm [427, **1**; 432, **2**; 438, **3**; 457 nm **4**] assignable to metal to ligand charge transfer (MLCT) transitions. Third one appeared in UV region at ~ 305 nm [319, **1**; 322, **2**; 304, **3**;339 nm **4**] and has been ascribed to dipyrrin based intra-ligand π–π* transitions [29–31].

3.6. Electronic absorption titration.

Electronic absorption spectroscopy is an effective tool to examine the binding mode of complexes with DNA by monitoring changes in absorption intensity and position of the bands. The absorption spectra have been recorded with a fixed concentration of **1**–**4** (10 μM) with increasing concentrations of CT DNA (0–20 μM) and resulting spectra is depicted in (Fig. S9). In case of complex **1** the band centered at 427 nm exhibited hypochromism (10%) with a small red shift of 4 nm and the weak band centered at 268 nm showed a hyperchromism (85%) with a red shift of 12 nm.Absorption spectraof**2** and **3**displayed similar changes under identical conditions(Fig S9). On the other hand, gradual addition of CT DNA to a solution of **4**led to hypochromism (8 and 6%) for the bands centered at 513 and 457 nm with small red shift of 2 nm. Further, appearance of a new band at 478 nm with apparent isosbestic points at 494 and 467 nm suggested existence of more than two species(Fig. 3). In addition, intra-ligand charge transfer transition centered at 281 nm displayed hyperchromism (70%) with blue shift of 3 nm and generation of a new shoulder at 336 nm with a clear isosbestic point at 390 nm. Observed spectral changes clearly revealed that complex **4** can interact with DNA through intercalation as well as groove binding *via* electrostatic interactions leading to DNA stabilization [20, 52].To

quantitatively compare DNA binding affinities intrinsic binding constant $K_b$has been calculated using the equation [53].

$$[DNA]/(\varepsilon_a - \varepsilon_f) = \frac{[DNA]}{\varepsilon_b - \varepsilon_f} + \frac{1}{k_b}(\varepsilon_b - \varepsilon_f) \text{..... (Eq. 1)}$$

where [DNA] is the concentration of DNA in base-pairs, ε_a is apparent extinction coefficient calculated as A_{obs}/[complex], ε_f corresponds to extinction coefficient of the complex in its free form and ε_b refers to extinction coefficient of the complex in bound form. Each set of data upon fitting in the above equation gives a straight line with a slope of 1/ ($\varepsilon_b - \varepsilon_f$) and a y-intercept of 1/K_b ($\varepsilon_b - \varepsilon_f$) and $K_b$was determined from the ratio of slope to intercept. The values of K_b varies in the order **4** (6 .5 × 10^4) >**3 (**5.5 × 10^4) >**2 (**2.2 × 10^4) >**1(**1.8 × 10^4).

3.7. Competitive binding between EB and complexes for CT DNA

Ethidium bromide (EB = 3,8-diamino-5-ethyl-6-phenyl-phenanthridiniumbromide) is a fluorescence dye having a planar structure that binds DNA in an intercalation mode. To affirm binding of **1**–**4**withDNA,competitive studieshave been performedusing DNA bound ethidium bromide (EB) by successive addition of 0–50 μM of complexes.Intercalation of the complexes with DNA causes decrease in binding sites of DNA available for EB, which in turn leads to a decrease in fluorescence intensity of the EB–DNA system [54–55]. The fluorescence emission intensity of DNA–EB system in presence of the compounds under investigation causes an appreciable lowering in fluorescence intensity upon increasing their amounts **(**by51.6%,**1**; 55.7%, **2**, 67.2%, **3** and 72%, **4**;(Fig. 4 and S10). From the data we conclude that **1**–**4** are capable of displacing EBfrom EB-DNA complex and strongly interact with DNA binding sites.The quenching parameters for **1**–**4** have been calculated using Stern–Volmer equation-

$$\frac{I_0}{I} = K_q[Q] + 1 \text{ ..... (Eq. 2)}$$

where I_0 and I represent emission intensities of EB-DNA in absence and presence of **1**–**4** respectively, K_q is the quenching constant and [Q] is concentration of **1**–**4**(Fig. S11).

The K_q values for **1**–**4** were found to be 1.22 × 10^4 M^{-1}, 1.33 × 10^4 M^{-1}, 1.66 × 10^4 M^{-1}, and 2.00 × 10^4 M^{-1}, respectively. Furthermore, apparent binding constant (K_{app}) values for the complexes have been deduced using following equation:

$$K_{EB}[EB] = K_{app}[complex] \text{ ..... (Eq. 3)}$$

where, [complex] is the value of decrease in the fluorescence intensity of EB at 50%, K_{EB} (1.0 × 10^7 M^{-1}) is binding constant of EB with CT DNA and [EB] presents the concentration of EB (10 μM). The apparent binding constants for **1**–**4** came out to be 3.2 × 10^4 M^{-1}, 3.4 × 10^4 M^{-1}, 6.4 × 10^4 $M^{-1}$and 8.2 × 10^4 M^{-1}, respectively and are comparable to earlier reports [20, 29–31].The above results suggest that **4** intercalated rather strongly than the other complexes whichis in good agreement with the UV–vis titration studies.

3.8. Partition coefficient determination.

Lipophilicity is an important physiological parameter in determining penetration behavior of drugs[56–57]. It has been estimated in terms of partition coefficient (log *P*) based on the amount of **1**–**4** dispersed in biphasic system (*n*–octanol/water) using the equation:

$$\log P = \log[Complex]_{octanol}/[Complex]_{water} \quad \text{..... (Eq. 4)}$$

The calculated log *P* values for**1**–**4** are 1.24, 1.26, 1.42 and 1.45,respectively(Table S1). Thelipophilicity of **4** and **3** are higher than **1** and **2**which may be attributed to presence of greater number of fluoro groups. The cytotoxicity increases with an increase in lipophilicity, therefore cytotoxicity of **4** and **3** should be higher than **1** and**2**, which has further been validated by MTT assay.

*3.9. Density functional theory calculations***.**

Geometry optimization for all the complexes under study has been carried out at DFT level. The rutheniummetal centre has been described by LANL2DZ basis set while non-metal atoms using 6-31G**. The starting geometries were taken from single crystal X-ray data for**4** and subjected to optimization employing Gaussview 5.0 and resulting coordinates have been energetically optimized. Calculated geometrical parameters such as bond lengths, bond angles and bond energies are consistent with single crystal X-ray data (Tables S2). Contour plots for some selected molecular orbitals of **1**–**4** were generated using Gauss view 5.0 and are shown in (Fig. 5). DFT calculations on**4** reproduced familiar "three-leg piano-stool" structures confirming the optimized structures for**1**–**3**(Fig 6 and S12).

From the DFT calculation it is clear that electron density of highest occupied molecular orbital (HOMO) is localized primarily on Ru atom, dipyrrin, and Cl^- ion whereas lowest

unoccupied molecular orbital (LUMO) mainly on dipyrrin and to some extent on phenyl unit. The calculated HOMO energies of the complexes are in the order of **1** (−5.22) <**2**(−5.11) >**3**(−5.35) <**4** (−5.22 eV) and those for LUMO exhibited the following trend: **1**(−2.01) ~**2**(−2.01) >**3**(−2.25) ~**4**(−2.25 eV). On the basis of DFT calculations and frontier molecular orbital theory, it is well established that DNA molecule acts as an electron donor and intercalated complex as electron acceptor [30, 58–59].In this regardenergy and population of LUMO of**1**–**4** could be considered as key factors for affecting DNA binding. As the number of fluoro substituent increases from **1**–**2** to **3–4** the LUMO energy of the complexes decreases which favours transfer of electron cloud from the HOMO of DNA towards LUMO of the complexes, indicating stronger interactions [60–64].The difference between the HOMO–LUMO in **1** (−3.21), **2** (−3.10), **3** (−3.10), and **4** (−2.97eV) are almost identical. At the basis of LUMO energy, the order of interaction of the complexesis**4 ~ 3 > 2 ~1**. The results arein good agreement with the experimental data and also number of important factors such as lipophilicity, H-bonding, steric bulk, rotational motion etc.which can also affect their biological activity [59,61].

*3.10. Molecular docking investigation on the interaction of DNA with **1**–**4***

Molecular docking has been established as an effective tool for rational drug designing through recognition of the drug–DNA interactions. The mechanism of action of reactants is ascertained by placing a small molecule into binding site of the target specific region of DNA, mainly in a noncovalent fashion, however a covalent bond may also be formed between the reactants. Binding mode varies depending upon structural properties of the reactants and molecular shape is believed to be the most important factor governing it. Earlier reports suggest that DNA–intercalator complex is stabilized *via* van der Waals forces, hydrogen bonding, hydrophobic charge transfer and electrostatic complementarity[31, 65].To predict preferred binding site along with orientation of the ligands inside the DNA minor groovedocking studiesusing **1**–**4** were performed with DNA duplex of the sequence d(CG-CGAATTCGCG)$_2$ dodecamer (PDB ID: 1BNA) [31]. Resulting model shows that compounds **1**– **4**recognise DNA in minor groove situated in the G–C rich region *via* electrostatic interaction. The planarity of dipyrrin core is comfortable for strong π–π stacking interactions which fits inside the DNA strands *via* van der Waals interaction and hydrophobic contacts (Fig. 7 and S13–S14, SI) [31,65].Moreover, fluorine atoms of **4** may be engaged in hydrogenbonding interactions with

DNA nucleobases available in the minor grooves in G–C rich region (Fig. S15). The docked structures for **1**–**4** with 1B-DNA exhibited relative binding affinity (–248.14, **1**; –249.34, **2**; –256.68, **3;**–263.57, **4**;eV**)** indicating **4** have better binding capability relative to other complexes under investigation. These results are in good agreement with the experimentalobservations.

3.11. Determination of IC_{50} value.

The cytotoxicity of ligands and complexes has been studied by MTT colorimetric assay against lung cancer cell line (A549). All the complexes induced cytotoxic response in a concentration dependent manner. On the basis of this assay, **4** exhibited the highest toxicity or lowest IC_{50} value followed by complex **3**, whereas **2** and **1** displayed poor toxicity and anti-proliferative activity against A549 cells. However, ligands did not show any toxicity up to 100μM concentration. The IC_{50} values are 20, **4**; 65–75, **3** and >100 μM**2**and**1**.On the basis of cytotoxicity it can be arranged as **4**>**3**>**2 > 1**(Fig.8) (Table S3). It is clearfrom the IC_{50} values that complex **4** is most efficient cytotoxic drug in comparison to others. Thus we have attempted further studies like changes in nuclear morphology, cell cycle analysis with the complex **4** only.

3.12. Change in nuclear morphology of cells.

Nuclear fragmentation is one of the prime features of apoptotic cell death.To investigate the cell death by apoptosis and changes in nuclear morphology, DNA binding dyes Hoechst and PI were used to investigate nucleus morphology of the control and treated cells.Hoechst is permeable to cell membrane and typically used to stain the nucleus of live/dead cells. Hoechst binds to the minor groove of double strand DNA preferably at AT rich regions and stains nucleus in blue colour.PI is usually used to identify the dead cells and it is membrane impermeable and gets excluded from viable cells. PI binds to DNA by intercalating between the bases without any sequence preference and gives red colour at respective wavelength.

In control cells, almost uniform level of blue fluorescent nuclei were seen which indicate that all cells are live and healthy. In treated cells, dead ones could be clearly visualized due to toxicity of the drugs and cell membrane disruption.At increasing concentrations of **4** early apoptotic cells with deep blue fluorescence (indicated with yellow circle), late apoptotic cells with fragmented nuclei (indicated with blue circle) and necrotic dead cells with red fluorescence (indicated with red circle) were clearly observed. At IC_{50} value (20 μM) of complex **4**

fragmented nuclei were clearly observed and it indicates that at this concentration above complex induced apoptosis very efficiently in A549 lung cancer cells (Fig.9).

3.13. Cell cycle analysis.

Cell death and cell cycle delay on the basis of DNA content, fluorescence activated cell sorting (FACS) was done with PI staining (Fig. 10). Cells were treated at three different concentrations (15, 20 and 25μM) of complex **4**. According to FACS histogram statistics, percentage of sub-G1 (apoptotic cell death) cells significantly increased from 2.67% to 32.8% in treated group as compared to control. Whereas at IC_{50} value, significant increase in G2/M phase of the cell cycle 18% to 25.57% were observed. On the other hand, in G1 phase cells were decreased from 71.67% to 38% while S phase was almost constant in control and treated group. Histogram statistics of FACS clearly indicated that complex **4** potentially induced apoptosis (increase in sub G1) as well as cell cycle delay (increase in G2/M) in A549.

4. Conclusions

In conclusion through this work a new set of organometallic complexes have been synthesized and thoroughly characterized by various physicochemical techniques. The DNA binding affinity of the complexes has been followed by spectrophotometric methods. The results supported interaction of the complexes with CT DNA through intercalation. Further, molecular docking studies suggest that these complexes bind with minor groove of DNA. Moreover, all the complexes (**1**–**4**) exhibited significant cytotoxicity toward A549 cell line with best performance from **4**, showing lowest IC_{50} value, prominent blebbing at low concentration (*c*, 20 μM).

Acknowledgements

Authors gratefully acknowledge financial support from the Department of Science and Technology (DST), New Delhi, India for providing financial assistance through the scheme [SR/S1/IC-25/2011] and also to CSIR, New Delhi, India for the award of a senior Research Fellowship to RPP (No. 09/013(0514)/2013-EMR-I). We are also thankful to the Head, Departments of Chemistry and Zoology,Institute of Science, Banaras Hindu University, Varanasi (U.P.) India, for extending laboratory facilities.We are also thankful to Prof. R. Murugavel (IIT

Bombay) for the access to his Single Crystal X-ray Diffraction Facility established through a DAE-SRC Outstanding Investigator Award.

Supporting Information

^{1}H, ^{13}C NMR, ESI-MS, UV−vis titration curves, fluorescence spectra, and Tables S1−S3 are provided.CCDC No. 1448655(**4**) contains the supplementary crystallographic data for this paper. It can be had free of charge via https://summary.ccdc.cam.ac. uk/structure-summary-form (or from the CCDC, 12 Union Road, Cambridge CB2 1EZ, U.K.; Fax: +44−1223−336033; Email: deposit@ccdc.cam.ac.uk).

Reference:

[1] T.C. Johnstone, J.J. Wilson, S. J. Lippard, Inorg. Chem.52(2013)12234–12249.

[2] N.J. Farrer, J.A. Woods, L. Salassa, Y. Zhao, K.S. Robinson, G. Clarkson, F.S. Mackay, P.J. Sadler, Angew. Chem. Int. Ed. 49 (2010) 8905–8908.

[3] P.J. Bednarski, F.S. Mackay, P.J. Sadler, AntiCancer Agents Med. Chem.7 (2007)75–93.

[4] C.G. Hartinger, N.M. Nolte, P.J. Dyson**,**Organometallics 31 (2012) 5677−5685.

[5]S.H. van Rijt, P.J. Sadler, Drug Discovery Today 14 (2009) 1089–1097.

[6] G.S. Fink,Dalton Trans. 39 (2010) 1673–1688 and references therein.

[7] A. A. Holder, Shawn Swavey, K. J. Brewer, Inorg. Chem.43 (2004) 303−308.

[8] S. Tabassum, M. Zaki, M. Ahmad, M. Afzal, S. Srivastav, S. Srikrishna, F. Arjmand,Eur. J. Med. Chem83 (2014) 141−154.

[9] R. A. Khan, A. Asim, R. Kakkar, D. Gupta, V. Bagchi, F.Arjmand, S.Tabassum,Organometallics 32 (2013) 2546−2551.

[10] S. Mukhopadhyay, R. K. Gupta, R. P. Paitandi, N. Rana, G. Sharma, B. Koch, L. K. Rana, M. S. Hundal, D. S. Pandey, organometalics 34 (2015) 4491−4506.

[11] A. Bergamo, C. Gaiddon, J. H. M. Schellens, J. H. Beijnen, G. Sava, J. Inorg. Biochem.106 (2012) 90.

[12] E. Antonarakis, A. Emadi, Cancer Chemother. Pharmacol.66 (2010) 1.

[13] V. Cepeda, M. A. Fuertes, J. Castilla, C. Alonso, C. Quevedo, J. M. Perez, Med. Chem.7 (2007)3.

[14] G. Giaccone, R.S. Herbst, C. Manegold, G. Scagliotti, R. Rosell, V. Miller, J.Clin.Onco*l*.22 (2004) 777−784.

[15] M. Clarke, J. Coord.Chem.Rev. 236 (2003) 209−233.

[16] G.S. Smitha, B. Therrien, Dalton Trans.40 (2011) 10793−10800.

[17] F. Lentz, A. Drescher, A. Lindauer, M. Henke, R.A. Hilger, C.G. Hartinger, M.E. Scheulen, C. Dittrich, B.K. Keppler, U. Jaehde, Anti-Cancer Drugs 20 (2009) 97.

[18] T. Gianferrara, I. Bratsos, E. Alessio, Dalton Trans. (2009) 7588–7598.

[19] H.K. Liu, P.J. Sadler Acc. Chem. Res. 44 (2011) 349–359.

[20] M. Ganeshpandian, R. Loganathan, E. Suresh, A. Riyasdeen, M.A. Akbarshad, M. Palaniandavar, Dalton Trans. 43 (2014) 1203–1219.

[21] M. Alagesan, N.S.P. Bhuvaneshb, N. Dharmaraj, Dalton Trans. 43 (2014) 15829– 15840.

[22] K.J. Kilpin, C.M. Clavel, F. Edafe, P.J. Dyson, Organometallics 31(2012) 7031−7039.

[23] A.Kumar, R.K. Gupta, A. Kumar, R. P. Paitandi, K. B. Singh, S. K. Trigun,M. S.Hundal, D S. Pandey. J. Organomet. Chem. 801 (2016) 68–79.

[24] P.U. Maheswari, M. Palaniandavar Journal of Inorganic Biochemistry 98 (2004) 219–230

[25] R.K. Gupta, R. Pandey, R. Singh, N. Srivastava, B. Maiti, S. Saha, P. Li, Q. Xu, D.S.Pandey, Inorg. Chem., 51(2012)8916–8930.

[26] B. Kilduff, D. Pogozhev, S.A. Baudron, M.W. Hosseini, Inorg. Chem., 49 (2010)11231−11239.

[27] S. A. Baudron, Dalton Trans 42 (2013) 7498–7509.

[28] K. Hanson, A. Tamayo, V.V. Diev, M.T. Whited, P.I. Djurovich, M.E. Thompson Inorg. Chem. 49 (2010) 6077–6084.

[29]R.K. Gupta, R. Pandey, G. Sharma, R. Prasad, B. Koch, S. Srikrishna, P.Z. Li, Q. Xu, D.S Pandey, Inorg.Chem.52 (2013)3687−3698.

[30] R.P. Paitandi, R.K. Gupta, R.S. Singh, G. Sharma, B. Koch, D.S. Pandey, Eur. J. Med. Chem. 84 (2014) 17–29.

[31] R.K. Gupta,G. Sharma, R. Pandey, A. Kumar, B. Koch, P.Z. Li, Q. Xu, D.S. Pandey. Inorg.Chem. 52 (2013) 13984−13996.

[32] F.M.D. Ismail, J. Fluorine Chem. 118 (2002) 27–33.

[33] B.E. Smart,J. Fluorine Chem. 109 (2001) 3–11.

[34]C. Isanbor, D. OHagan, J. Fluorine Chem. 127 (2006) 303–319.

[35] P.V. Danenberg, Frontiers Biosci. 9 (2004) 2484–2494.

[36] D.D. Perrin, W.L.F. Armango, D.R. Perrin, Purification of laboratory Chemicals; Pergamon: Oxford, U.K. 1986.

[37] M.A. Bennett, A.K. Smith, J. Chem. Soc., Dalton Trans. (1974) 233–241.

[38] P. Crochet, B. Demerseman, C. Rocaboy, D. Schleyer, Organometallics. 15 (1996) 3048–3061.

[39] B.J. Littler, M.A. Miller, C.H. Hung, R.W. Wagner, D.F. O'Shea, P.D. Boyle, J.S. Lindsey J. Org.Chem. 64 (1999)1391–1396.

[40] G.M. Sheldrick, Acta cryst. A 64(2008) 112.

[41] A.L. Spek, PLATON, A Multipurpose Crystallographic ToolsUtrecht University, Utrecht, The Netherlands, (2000).

[42] A.L. Spek, Acta Crystallogr. A46 (1990) C31.

[43] D. Mustard, D.W. Ritchie, Proteins*:* Struct. Funct.Bioinf. 60 (2005) 269

[44] M.J. Frisch, G.W. Trucks, H.B. Schlegel, G.E. Scuseria, M.A. Robb, J.R. Cheeseman, G. Scalmani, V. Barone, B. Mennucci, G.A. Petersson, H. Nakatsuji, M. Caricato, X. Li, H.P. Hratchian, A.F. Izmaylov, J. Bloino, G. Zheng, J.L. Sonnenberg, M. Hada, M. Ehara, K. Toyota, R. Fukuda, J. Hasegawa, M. Ishida, T. Nakajima, Y. Honda, O. Kitao, H. Nakai, T. Vreven, J.A. Montgomery, Jr., J.E. Peralta, F. Ogliaro, M. Bearpark, J.J. Heyd, E. Brothers, K.N. Kudin, V.N. Staroverov, R. Kobayashi, J. Normand, K. Raghavachari, A. Rendell, J.C. Burant, S.S. Iyengar, J. Tomasi, M. Cossi, N. Rega, J.M. Millam, M. Klene, J.E. Knox, J.B. Cross, V. Bakken, C. Adamo, J. Jaramillo, R. Gomperts, R.E. Stratmann, O. Yazyev, A.J. Austin, R. Cammi, C. Pomelli, J.W. Ochterski, R.L. Martin, K. Morokuma, V.G. Zakrzewski, G.A. Voth, P. Salvador, J.J. Dannenberg, S. Dapprich, A.D. Daniels, Ö. Farkas, J.B. Foresman, J.V. Ortiz, J. Cioslowski, and D.J. Fox, Gaussian 09, revision A.1, Gaussian, Inc., Wallingford, CT, 2009.

[45] A.D. Becke J. Chem. Phys. 98 (1993) 5648.

[46] W.R. Wadt, P. Hay, J. Chem. Phys. 82 (1985) 284.

[47] M.V. Berridge, P.M. Herst, A.S. Tan, Biotech. Ann. Review.11 (2005) 127–152.

[48]U. Ziegler P. Groscurth Morphological features of cell death. News Physiology Sci. 19 (2004) 124–128.

[49] T. Bezabeh, M.R.A. Mowat, L. Jarolim, A.H Greenberg, I.C.P. Smith. Death and Differentiation 8 (2001) 219–224.

[50] C. Riccardi, I. Nicoletti, Nat Protoc. 3 (2006) 1458–61.

[51] A. Dorcier, P.J. Dyson, C. Gossens, U. Rothlisberger, R. Scopelliti, I. Tavernelli, organometalics 24 (2005) 2114–2123.

[52] M.A. Rizvi, M. Zaki, M. Afzal, M. Mane, M. Kumar, B.A. Shah, S. Srivastav, S. Srikrishna, G.M. Peerzada, S.Tabassum, Eur. J. Med. Chem 90 (2015) 876–888.

[53] A. Wolfe, G.H. Shimer, T. Meehan, Biochemistry 26 (1987) 6392–6396.

[54] R.F. Pasternack, E.J. Gibbs, J.J. Villafranca, Biochemistry. 22 (1983) 251.

[55] Z.C. Liu, B.D. Wang, Z.Y.Yang, Y. Li, D.D. Qin, T.R. Li, Eur. J. Med. Chem. 44 (2009) 4477.

[56] OECD, Guidelines for Testing of Chemicals. In OECD; Paris, 107 (1995).

[57] L.P. Graham, An Introduction to Medicinal Chemistry; Oxford University Press: Oxford, UK, 1995.

[58] K. Fukui, T. Yonezawa, H. Shingu, J. Chem. Phys. 20 (1952) 722.

[59] I. Fleming, Frontier Orbital and Organic Chemical Reaction, Wiley, New York, 1976.

[60] X.H. Zou, B.H. Ye, H. Li, Q.L. Zhang, H. Chao, J.G. Liu, L.N. Ji, X.Y. Li, J. Biol. Inorg. Chem. 6 (2001) 143–150.

[61] N. Kurita, K. Kobayashi, Comput. Chem. 24 (2000) 351–357.

[62] X.W. Liu, J. Li, H. Deng, K.C. Zheng, Z.W. Mao, L.N. Ji,Inorg. Chim. Acta 358 (2005) 3311–3319.

[63] G. Klopman, J. Am. Chem. Soc. 90 (1968) 223–234.

[64] L.M. Chen, J. Liu, J.C. Chen, C.P. Tan, S. Shi, K.C. Zheng, L.N. Ji, J. Inorg. Biochem. 102 (2008) 330–341.

[65] S. Tabassum, M. Zaki, M. Afzal, F. Arjmand, Dalton Trans.42 (2013) 10029–10041.

Table 1. Crystal data and structure refinement parameters for **4**

Empirical formula	$C_{27}H_{24}ClF_5N_2Ru$
Crystal system	Monoclinic
Space group	$P2_1/n$
a (Å)	7.3790(18)
b (Å)	14.783(4)
c (Å)	23.820(6)
α (deg)	90.00
β (deg)	92.972(4)
γ (deg)	90.00
V (Å^3), *Z*	2594.9(11), 4
λ (Å)	0.71075
Colour and habit	Red, needle
T (K)	150(2)
reflns collected	19435
refins/restraint/params	4562/0/325
D_{calcd} (Mg m^{-3})	1.647
μ (mm^{-1})	0.762
GOF on F^2	1.149
final *R* indices $I>2\sigma(I)$	R1 = 0.0486
	wR2 = 0.0971
R indices (all data)	R1 = 0.0522
	wR2 = 0.0990

Table 2 Selected bond lengths (Å) and angles (°) for **4**

Bond length (Å)	**4**	**Bond Angle (°)**	**4**
Ru–N1	2.0628	N2–Ru1–N1	83.87
Ru–N2	2.0715	N2–Ru1–Cl1	87.24
Ru–Cl1	2.4134	N1–Ru1–Cl1	88.72
Ru–C*g*	1.6738	C*g*–Ru–Cl1	126.87
Ru–C*av*	2.182	C*g*–Ru–N1	127.71
		C*g*–Ru–N2	128.28

C*g*= metal centroid bond distance, C*av* = average metal-carbon bond distance.

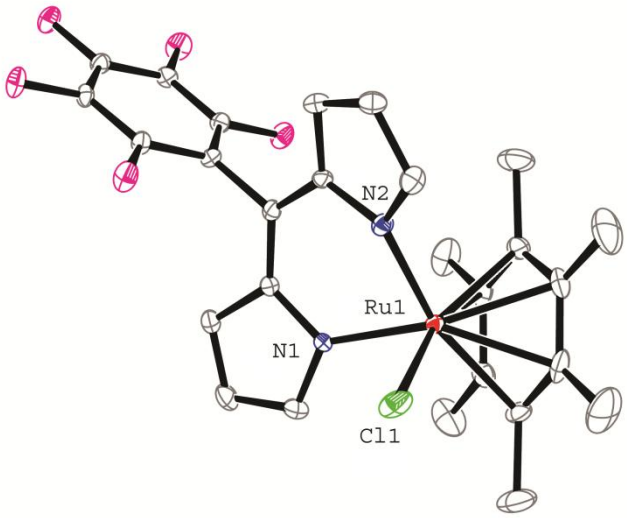

Fig. **1**. ORTEP views of **4** at 30% thermal ellipsoid probability (Solvent molecule and H-atoms have been omitted for clarity).

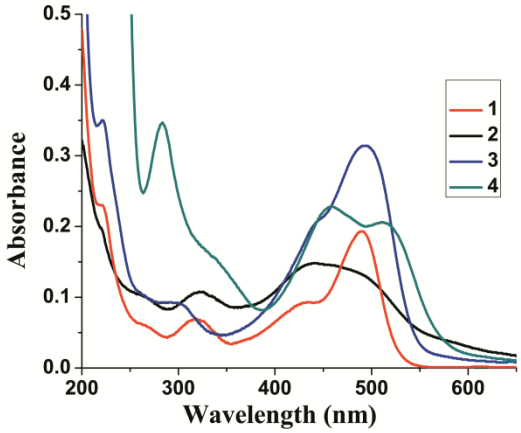

Fig. 2. Electronic spectra of ligand and complexes **1**–**4** in ((EtOH:H_2O, *c*, 10 μM; 1:1, v/v; *p*H ~7.3).

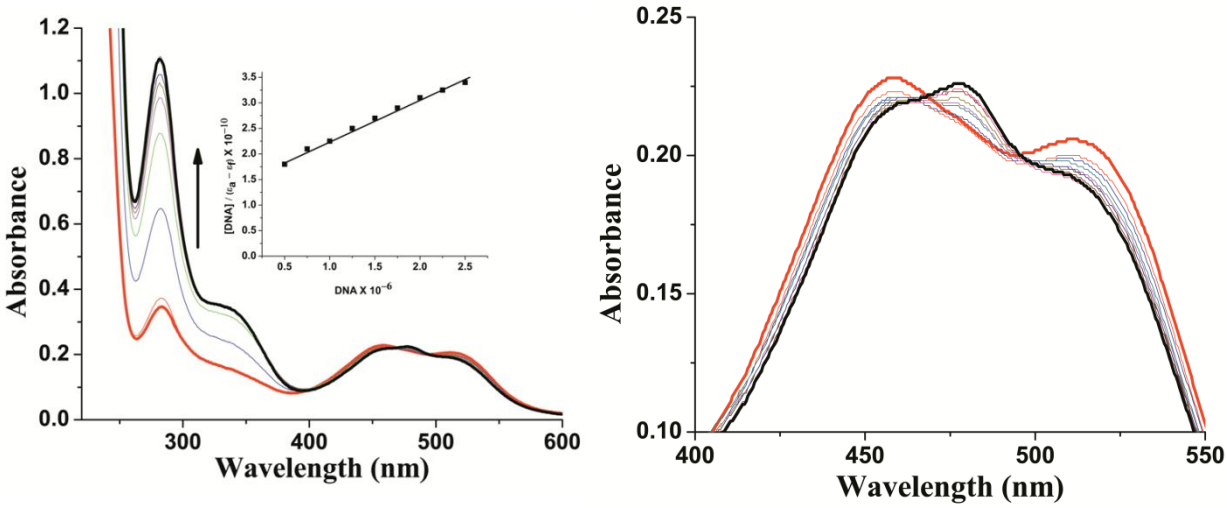

Fig. **3**.Absorption titration spectra of **4** (EtOH:H_2O, *c*, 10 μM; 1:1, v/v; pH ~7.3) in the absence **(**red line**)** and presence (other lines) of CT DNA (1–20 μM) at room temperature. Arrow shows the changes in absorption intensity upon increasing the CT DNA concentration.

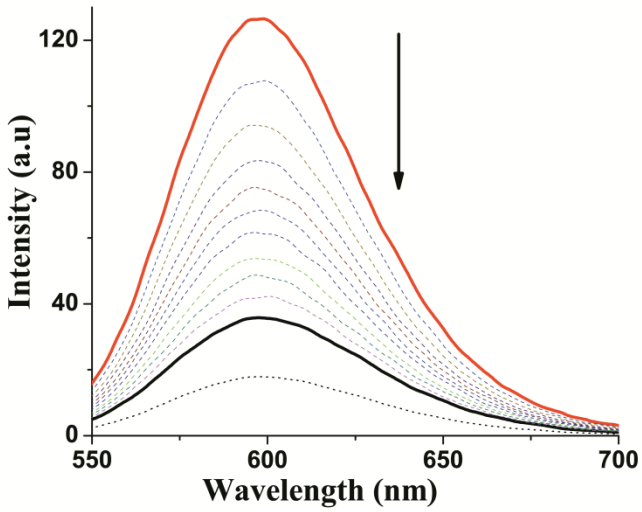

Fig. **4**. Emission spectra of EB (dotted black line) EB bound to CT DNA (Red solid line) and in presence (other lines) of **4 (**withincreasing amounts 0–50 μM). [EB] = 10 μM, [CT DNA] = 10 μM.

COM.	HOMO	LUMO
1	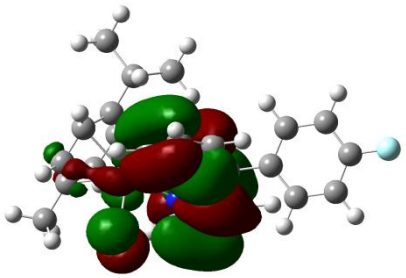	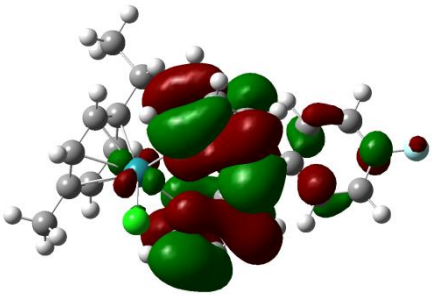
2	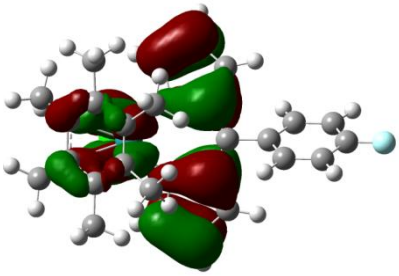	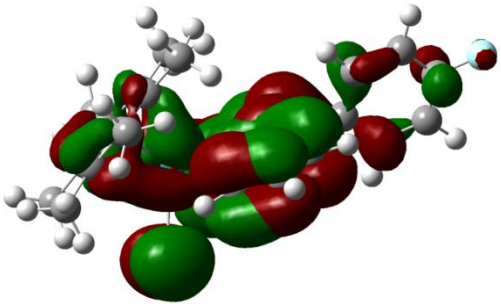
3	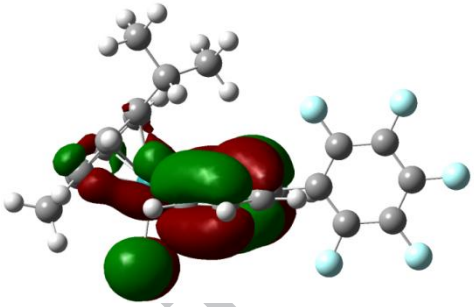	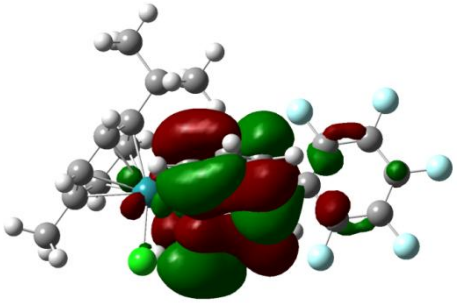
4	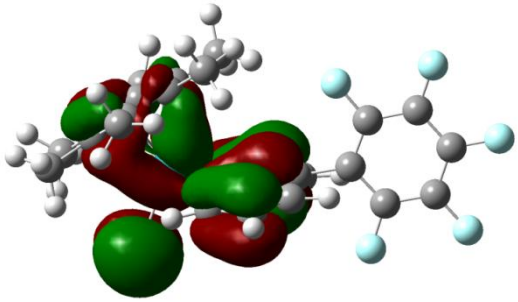	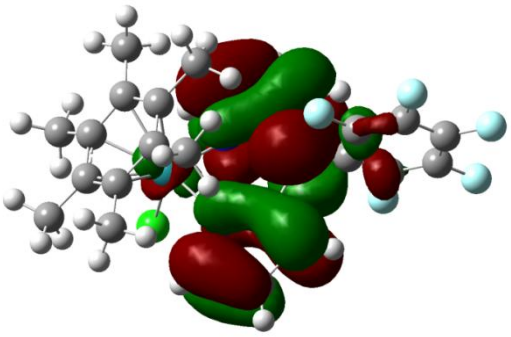

Fig.5. Frontier MOs contour plots of complex **1–4.**

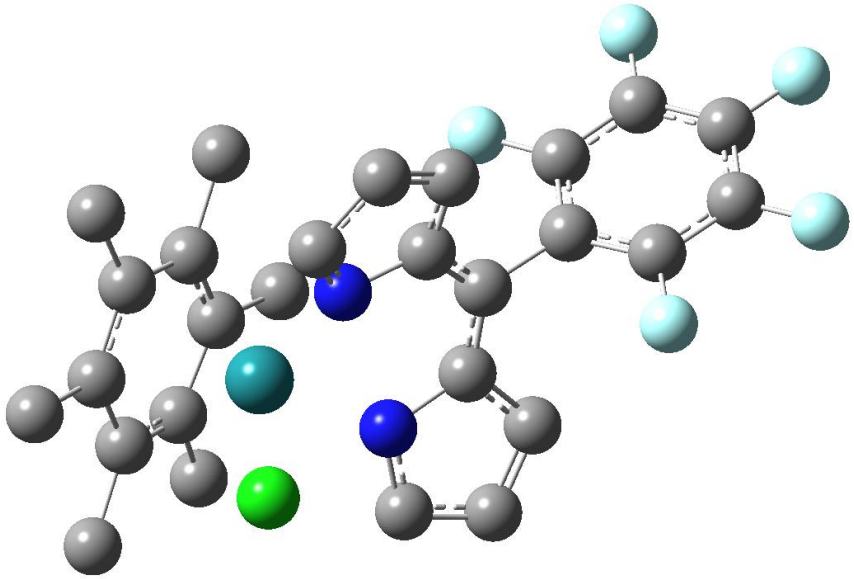

Fig. 6.DFT optimised structure of complex **4**

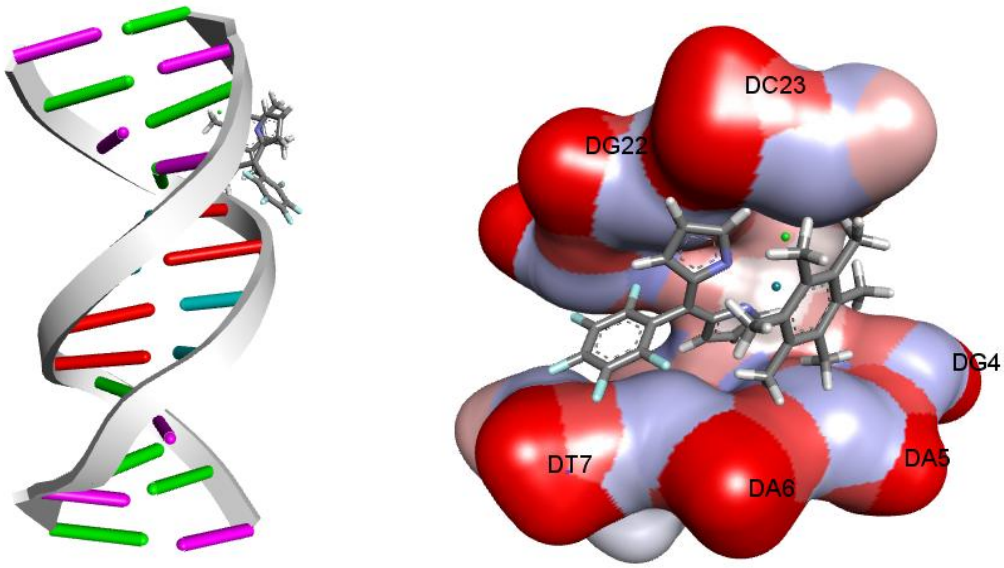

Fig. 7. Molecular docked model of complex **4** with DNA (PDB ID: 1BNA).

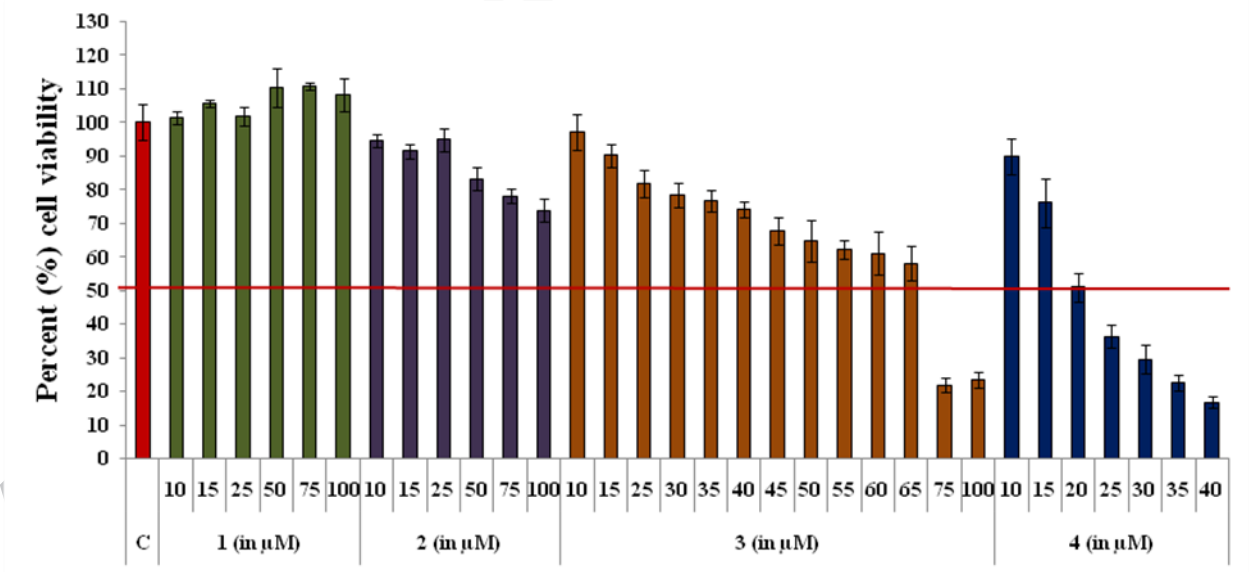

Fig. 8. Cell viability and antiproliferation profile of complex **1**–**4** against A549 lung cancer cells after drug treatment for 24 h by MTT assay.

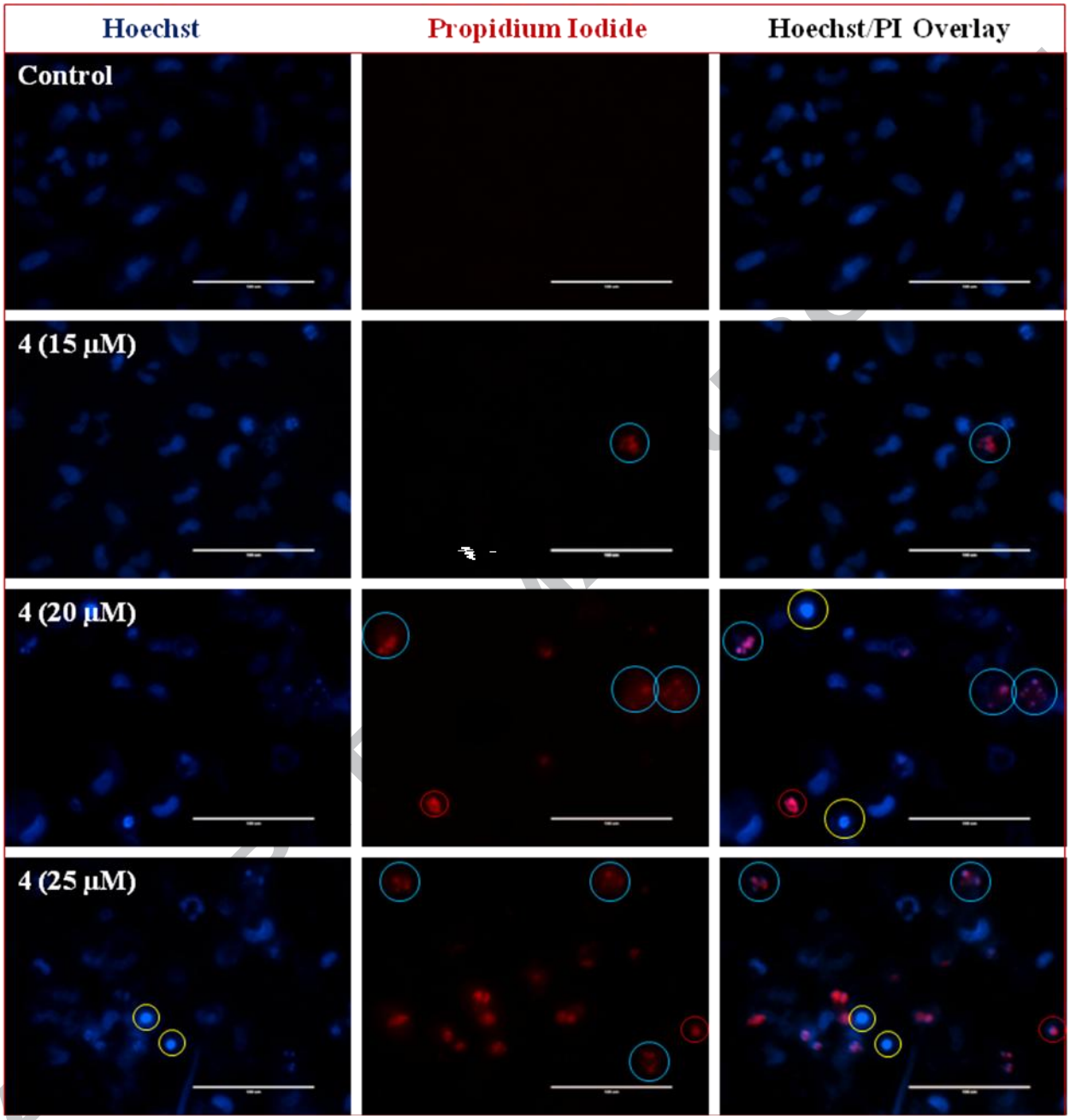

Fig. 9. Images of control and drug treated A549 lung cancer cells with Hoechst and PI staining after 24 h of incubation with three different concentrations of complex **4**. Early apoptotic cells indicated with yellow circle, late apoptotic cells with fragmented nucleus indicated with blue circle and necrotic dead cells with red fluorescence indicated with red circle.

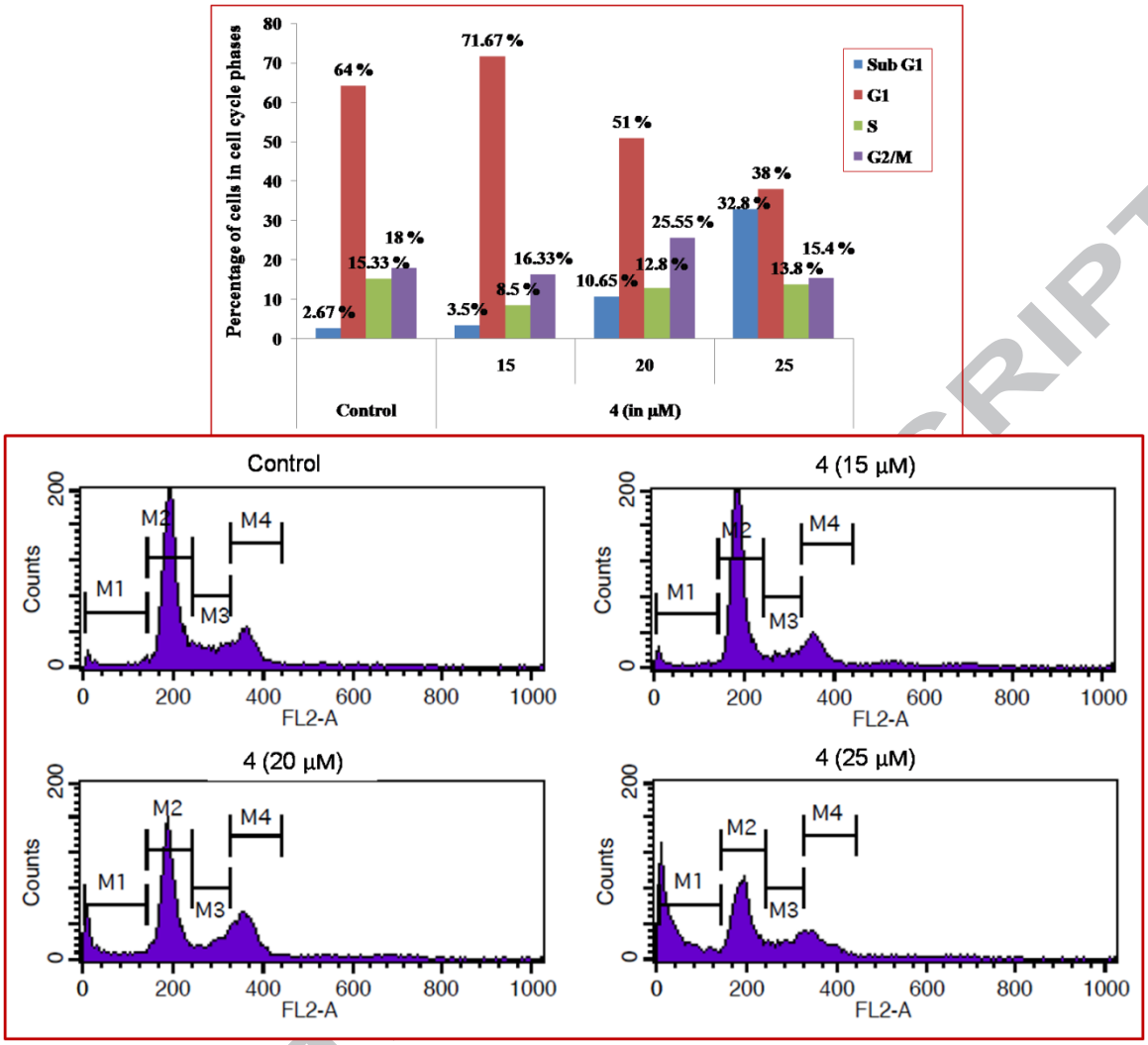

Fig.10.Control and treated A549 cells with **4** with 3 different concentrations including their IC_{50} value. The cells were fixed, stained with Propidium Iodide (PI) and analyzed by FACScan using Cell Quest software (Becton Dickinson).

Graphical abstract

Synthesis of four new arene ruthenium(II) complexes [(η^6-$C_{10}H_{14}$)RuCl(MFPdpm)] (**1**); [(η^6-$C_{12}H_{18}$)Ru-Cl(MFPdpm)] (**2**); [(η^6-$C_{10}H_{14}$)RuCl(PFPdpm)] (**3**) and [(η^6-$C_{12}H_{18}$)RuCl(PFPdpm)] (**4**) containing dipyrrin ligands 5-(4-fluoro)phenyldipyrromethene (MFPdpm) and 5-(penta-fluoro)phenyldipyrromethene (PFPdpm) have been described. DNA binding activities of **1**–**4** have been investigated by UV−vis and fluorescence spectroscopy and their binding through the minor groove of DNA has been established by molecular docking studies. The complexes **1**–**4** exhibit significant cytotoxicity toward human lung cancer cell line (A549).

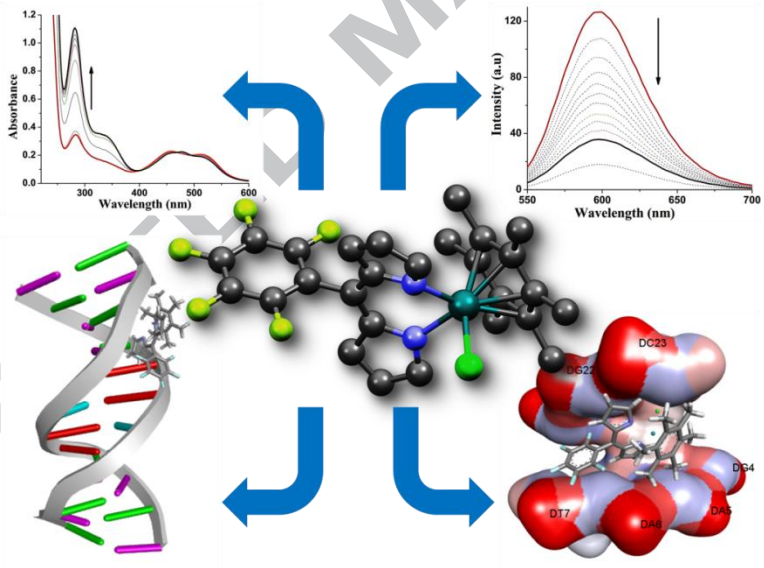

Highlights

1. Synthesis and characterization of arene ruthenium (II) complexes based on fluoro-dipyrrins ligands.
2. A comparative study towards DNA binding affinity of these arene ruthenium (II) complexes.
3. Establishment of the investigated complexes as potential anticancer agents.